A STABLE AND IMPROVED VERSION OF THE GFEM FOR THE ANALYSIS OF PROBLEMS IN ELASTIC LINEAR FRACTURE

Caio S. Ramos
Murilo H. C. Bento
Sergio P. B. Proença
caio_silva@usp.br
m.bento@usp.br
persival@sc.usp.br
Department of Structural Engineering, São Carlos School of Engineering, University of São Paulo
Avenida Trabalhador São Carlense, 400, 13566-590, São Paulo/São Carlos, Brazil

Abstract. Currently the Generalized Finite Element Method (GFEM) has been widely applied in the modeling of localized solids failures. Its main advantage consists of the expansion of the Finite Element Method (FEM) approach space by inserting functions (known as enrichment functions) that best locally represent the behavior of the searched solution. Such functions may have specific characteristics or even be generated numerically. On the one hand, the GFEM provides optimal convergence, however, it is prone to introduce linear dependencies into its system of equations, making the matrix ill-conditioned or even singular. The so-called stable version of the Generalized Finite Element Method (SGFEM) explores a modification in the enrichment functions to improve the conditioning of the stiffness matrix. However, such a modification leads to loss of precision in problems such as strong discontinuities. In order to reconcile the incompatibility between the solution precision and the system matrix conditioning, this work addresses a new modification of the space of GFEM shape functions associated with enrichment: flat-top functions as Partition of Unit (PU) and a new PU based on trigonometric functions, these are used exclusively in the construction of enriched shape functions. This new version of the GFEM presents a system matrix conditioning almost insensitive to the mesh / discontinuity configuration, even if the crack path approaches the element nodes. In addition, for flat-top PU with a small stabilization parameter, this version is almost of the same precision as the GFEM. Since only the PU is modified, the presented proposal can be easily implemented in pre-existing GFEM codes. Several representative numerical simulations of benchmark tests are presented to validate the proposal, considering both the accuracy of the solution and the conditioning of the system matrix.

Keywords: GFEM, Flat-top PU, Trigometric PU, Scaled Condition Number, Strong discontinuities.

1 Introduction

In the last two decades several researches have demonstrated the effectiveness of the Generalized Finite Element Method (GFEM) in solving problems with localized features as singularities and discontinuities aa. The main concept of the GFEM is to incorporate the a priori knowledge of the behavior of the solution in the approximation space, exploring the Partition of Unity (PoU) structure of the Finite Element Method (FEM). In this way, for example, it is possible to account for a strong discontinuity within a finite element by including of discontinuous functions in the so called enrichment space of approach. Such characteristics provide flexibility as well a significant improvement in numerical accuracy compared to FEM.

However, the unrestricted increasing of the approximation space can introduce ill conditioning in the GFEM system of equations due to the lack of linear independence of the set of shape functions. As a consequence, round-off errors can assume strong deleterious effects over the quality and representativeness of the numerical solution. Babuška and Banerjee [1, 2] mathematically demonstrate, for regular meshes with h refinement, that the condition number of the stiffness matrix grows at a rate of $\mathcal{O}(h^{-4})$ even when a non-polynomial function is used as enrichment. Such a result is much worse compared to the FEM where growth rate is of $\mathcal{O}(h^{-2})$. This GFEM drawback can sometimes represent an important constraint, especially in solving nonlinear problems due to the accumulation of rounding errors, and convergence problems in iterative linear solvers as shown Béchet et al. [3] and Fries and Belytschko [4]. Several studies propose methodologies for the solution of this adversity, for example, Béchet et al. [3], Laborde et al. [5] and Menk and Bordas [6], but with limited success.

In addition, when local expansion of the approximation space result from enrichment limited to a certain portion of the domain it may occur so-called blending elements, that is, elements containing enriched and unenriched nodes, which do not reproduce completely the enrichment function. The presence of these elements penalizes the approximate solution convergence rate, as shown by Laborde et al. [5], Chessa et al. [7], Fries [8], Gracie et al. [9], Tarancón et al. [10] and Shibanuma and Utsunomiya [11]. Several approaches to solve this problem are found in the literature, for example in Chessa et al. [7], Fries [8] and Shibanuma and Utsunomiya [11]. However, implementation of these approaches in pre-existing GFEM codes is not simple and optimal convergence is not always guaranteed, as shown in Aragón et al. [12].

The drawback cited above was recently addressed by Babuška and Banerjee [1, 2], who proposed a modification in the enrichment function that minimizes this problem. The version of GFEM incorporating this modification has been referred to as the Stable Generalized Finite Element Method (SGFEM). Such modification aims to create an enriched shape function space that is almost orthogonal to the FEM approximation space while preserving GFEM flexibility and convergence features. Babuška and Banerjee [1, 2] mathematically demonstrate that the stiffness matrix conditioning of the SGFEM grows at a rate of $\mathcal{O}(h^{-2})$, that is, about the same order as the FEM.

However, Gupta et al. [13] and Gupta et al. [14] observed that the direct extension of the idea presented by Babuška and Banerjee [1, 2] does not guarantee optimal convergence for two-dimensional and three-dimensional crack problems. The optimal convergence order is retrieved in Gupta et al. [13] and Gupta et al. [14] employing additional regularizations to the discontinuity functions. Later on, Zhang et al. [15] and Zhang et al. [16] point out that the strategy employed by Gupta et al. [13] and Gupta et al. [14] still does not guarantee robust conditioning in relation to the relative position of the crack line to the mesh.

Investigating the properties of the so-called higher order SGFEM, Zhang et al. [17] demonstrate that for enrichments with higher degree polynomial functions (>2), the firstly suggested modification imposed on the enrichment functions is not a sufficient condition to guarantee a good conditioning of the solving system. Thus, a further modification to be applied to the enrichment space is proposed, and is equivalent to the replacement of the conventional FEM PoU functions (hat-functions) by the flat-top PoU. From one-dimensional numerical analysis, Zhang et al. [17]demonstrate that the new modification ensures local linear independence between the FEM approach space and the enrichment space. These
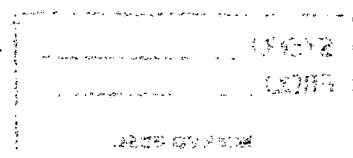
authors refer to this new version of GFEM as High Order SGFEM due to higher convergence rates obtained (>2).

Recently, Sato [18] and Sato et al. [19], based on the suggestion given Zhang et al. [17], extended the flat-top PoU formulation to two-dimensional analyses and, through quadrilateral finite element discretization obtained results that showed good conditioning as a consequence of the linear independence between the FEM approximation space and the enrichment function space. Similarly, Ramos and Proença [20] and Ramos [21] extend the flat-top PoU formulation to triangular finite elements then obtaining stable results with optimum rates of convergence. However, despite analyzing crack domain problems, these authors did not address the robustness of the condition number with respect to the crack position relative to the mesh geometry.

This paper adresses that issue as well in the context of two-dimensional analysis from the perspective of quadrilateral finite element discretization. Therefore, constituting original contributions, we formulate a new PoU based on trigonometric functions for quadrilateral finite elements. Moreover, it is demonstrated that the exclusive use of flat-top PoU only does not satisfy the robustness condition in relation to the relative position of the crack line. In this context, we present a new methodology based on the previous selection of which enrichment each PoU will be applied to. Thus, a broader version of GFEM is obtained, which considers any enrichment functions as well as different PoUs.

2 Model Problem

In this study, it is considered a domain $\bar{\Omega} = \Omega \cup \partial\Omega \in \mathbb{R}^2$ of elastic and cracked linear behavior. In the absence of volume forces, the equilibrium equation and the constitutive relations for the problem are defined as:

$$\nabla \cdot \boldsymbol{\sigma} := 0 \quad \boldsymbol{\sigma} := \mathfrak{C} : \boldsymbol{\varepsilon} \quad \text{in } \Omega, \tag{1}$$

where $\boldsymbol{\sigma}$ is denoted Cauchy tension tensor, $\mathfrak{C}$ is Hooke's constitutive tensor and $\boldsymbol{\varepsilon}$ it is the tensor of small deformations. Then Neumann boundary conditions are defined over $\partial\Omega$ such that,

$$\bar{t} := \boldsymbol{\sigma} \cdot \boldsymbol{n} \tag{2}$$

where $\boldsymbol{n}$ is the external normal unit vector of $\partial\Omega$, $\bar{t}$ are prescribed external distributed loading. It is assumed that the crack surface is free of loads. In our simulations Dirichlet boundary conditions are pointwise imposed in order to eliminate rigid body displacements. Through the Equations (1) and (2) the strong form is defined.

Weak formulation reduces strong continuity requirements over test functions, thus enabling to look for approximate solutions in an enlarged space, Proença [22]. In this context, the weak form is defined through the Principle of Virtual Work, that states: Find $\boldsymbol{u} \in H^1(\Omega)$ such that $\forall v \in H^1(\Omega)$

$$B(\boldsymbol{u}, \, \boldsymbol{v}) := F(\boldsymbol{v}) \tag{3}$$

where,

$$B(\boldsymbol{u}, \, \boldsymbol{v}) := \int_\Omega \boldsymbol{\sigma}(\boldsymbol{u}) : \boldsymbol{\varepsilon}(\boldsymbol{v}) \, d\Omega,$$
$$F(\boldsymbol{v}) := \int_{\partial\Omega} \bar{t} \cdot \boldsymbol{v} \, d(\partial\Omega), \tag{4}$$

where, u and v are *test* functions belonging to the Hilbert space $H^1(\Omega)$. Thus, for the problem under analysis, using the Galerkin method can be applied to find an approximation u_h of the exact solution u defined in Equation (3) and belonging to a finite dimensional space. Therefore, the discretized problem consists on: Find $u_h \in \mathcal{S}(\Omega)$ such that $\forall v_h \in \mathcal{S}(\Omega)$

$$\int_\Omega \sigma(u_h) : \varepsilon(v_h) \, d\Omega = \int_{\partial\Omega} \bar{t} \cdot v_h \, d(\partial\Omega) \tag{5}$$

Formally, by using the Galerkin method, a subspace $\mathcal{S}(\Omega)$ of $H^1(\Omega)$ is adopted that contain approximation functions (*test*) of the exact solution. Therefore, $\mathcal{S}(\Omega) \subset H^1(\Omega)$, and depends on the numerical method used to construct the approximation. In the following sections we demonstrate the construction of numerical approximations through the approximation spaces provided by GFEM and SGFEM.

3 On the GFEM and SGFEM

The GFEM is a Galerkin method whose approximation space is obtained by expanding the FEM approximation space with special functions that well approximate locally the solution of the problem under analysis. Such expansion is built by exploiting the PoU properties of the shape functions of the FEM. In short, the shape functions of GFEM are constructed by the product between PoU φ_i provided by the FEM elements and the enrichment functions, i.e.,

$$\varphi_i \times \boldsymbol{L}_i \tag{6}$$

Let, $I_h = \{0, \ldots, N\}$ the set of indexes of discretization nodes adopted on finite elements of dimension h and N the number of nodes, $i \in I_h^e \subset I_h$ such that I_h^e is the set with the node indexes of the elements e belonging to *cloud/patch* ω_i and $\boldsymbol{L}_i$ is the $n_i + 1$ dimension vector which contain enrichment functions $\psi_j^{(i)}$ linked to the ω_i *cloud*, that is,

$$\boldsymbol{L}_i = \{\psi_j^{(i)} : 0 \le j \le n_i, \ \psi_j^{(i)} \in H^1, \ \psi_0^{(i)} = 1\}, \tag{7}$$

where n_i is a nonnegative integer tied to the amount of cloud-bound ω_i enrichment functions.

In GFEM, φ_i, $i \in I_h$, are linear and bilinear lagrangian functions with defined *cloud* support ω_i, i.e., the *patch* defined by the elements sharing the same node i, Oden and Duarte [23]. According to Melenk [24], such functions constitute a PoU, because they agree with the unit sum property, that is, $\sum_{i \in I_h} \varphi_i(x) = 1$, $\forall x \in \bar{\Omega}$, and ensure conformity to the global approximation obtained.

Therefore, in terms of a general representation, the GFEM test function space is defined by the Equation (6) that,

$$\mathcal{S} = \sum_{i \in I_h} \varphi_i \boldsymbol{L}_i \boldsymbol{b}_i = \{\varphi_i \psi_j^{(i)} b_j^{(i)} : 0 \le j \le n_i, \ i \in I_h\} := \mathcal{S}_1 + \mathcal{S}_2, \tag{8}$$

where,

$$\mathcal{S}_1 = \{\zeta : \zeta = \sum_{i \in I_h} \varphi_i \psi_0^{(i)} b_0^{(i)}\}, \quad \mathcal{S}_2 = \{\zeta : \zeta = \sum_{i \in I_h} \sum_{j=1}^{n_i} \varphi_i \psi_j^{(i)} b_j^{(i)}\}. \tag{9}$$

$b_0^{(i)}$, $b_j^{(i)} \in \mathbb{R}$ and represent the degrees of freedom tied to the nodes of the discretization mesh. $\mathcal{S}_1$ refers to the approach space of the FEM and $\mathcal{S}_2$ to the space of enriched shape functions. Note that for *patches* ω_i where $n_i = 0$ the local approach space $\mathcal{S}$ it's the same as FEM.

Proposed by Babuška and Banerjee [1, 2], in the hereby denoted *Classical* SGFEM , GFEM enrichment functions are locally modified to make them null on *patch* nodes ω_i. This can be done through the following transformation:

$$\overline{\psi}_j^{(i)} := \psi_j^{(i)} - \mathcal{I}_{\omega_i}\left(\psi_j^{(i)}\right), \tag{10}$$

where, for two dimensional problems,

$$\mathcal{I}_{\omega_i}\left(\psi_j^{(i)}\right) := \sum_{k \in I_h^e} \varphi_k \psi_j^{(i)}(x_k, y_k)\big|_{\omega_i}. \tag{11}$$

$\overline{\psi}_j^{(i)}$ is the modified enrichment function, $\mathcal{I}_{\omega_i}\left(\psi_j^{(i)}\right)$ is an interpolation of the nodal values of $\psi_j^{(i)}$ over the *patch* ω_i and (x_k, y_k) are the coordinates of node k.

With the modification obtained, the same procedure presented in Equation (8) is used to construct SGFEM approximation spaces, resulting in,

$$\mathcal{S} = \sum_{i \in I_h} \varphi_i \overline{L}_i b_i = \mathcal{S}_1 + \bar{\mathcal{S}}_2, \quad \bar{\mathcal{S}}_2 = \{\zeta : \zeta = \sum_{i \in I_h} \sum_{j=1}^{n_i} \varphi_i \overline{\psi}_j^{(i)} b_j^{(i)}\}. \tag{12}$$

As mentioned earlier, although the expectation of optimal convergence is an excellent feature of GFEM, to obtain it is important that the resulting system of equations can be accurately and efficiently solved, in other words, the system of equations must be well conditioned. The scaled condition number $\mathfrak{K}(K)$ as an indicator of matrix conditioning, defined from the condition number $\kappa_2(\cdot)$ of the scaled matrix $\hat{K}$, as shown below:

$$\mathfrak{K}(K) := \kappa_2(\hat{K}) = \kappa_2(DKD) = \|\hat{K}\|_2 \|\hat{K}^{-1}\|_2, \tag{13}$$

where, D is a diagonal matrix with $D_{ii} = K_{ii}^{-1/2}$ and $\|\cdot\|_2$ is the Euclidean norm.

Babuška and Banerjee [1, 2] demonstrate mathematically for one-dimensional problems enriched with polynomial functions that $\mathfrak{K}(K_{GFEM}) = \mathcal{O}(h^{-4})$ and $\mathfrak{K}(K_{SGFEM}) = \mathcal{O}(h^{-2})$, that is, the conditioning of the SGFEM, in contrast to that of the GFEM, is of the same order of magnitude as the FEM. However, Zhang et al. [17] state that the modification imposed by the SGFEM on enrichment functions is not a sufficient condition to guarantee that there will be no linear dependencies. Therefore, these authors suggest a second modification on $\bar{\mathcal{S}}_2$ in order to ensure local linear independence of space $\mathcal{S}_1$. This change ultimately translates into the use of distinct PoUs for the construction of spaces $\mathcal{S}_1$ and $\bar{\mathcal{S}}_2$. Thus, similar to that construction presented in Equation (8), SGFEM approximation space is now defined as,

$$\mathcal{S} := \mathcal{S}_1 + \bar{\mathcal{S}}_2^{mod}, \tag{14}$$

where,

$$\mathcal{S}_1 = \{\zeta : \zeta = \sum_{i \in I_h} \varphi_i \psi_0^{(i)} b_0^{(i)}\}, \quad \bar{\mathcal{S}}_2^{mod} = \{\zeta : \zeta = \sum_{i \in I_h} \sum_{j=1}^{n_i} \varphi_i^* \overline{\psi}_j^{(i)} b_j^{(i)}\}. \tag{15}$$

φ_i^* is a special PoU applied only to construct the enrichment space. In subsection 3.1 two types of PoU φ_i^* are suggested that will be the object of study of this paper. Such partitions are denoted: flat-top PoU and trigonometric PoU.

Throughout the remainder of this work, SGFEM versions will be referred to in accordance with the PoU adopted to build the $\bar{\mathcal{S}}_2^{mod}$. Thus, SGFEM^{FT} refers to the version that uses flat-top PoU and SGFEM^{TRIG} when employed trigonometric PoU.

3.1 Special Partitions of Unity

The flat-top PoU was initially studied by Griebel and Schweitzer [25], Schweitzer [26, p. 97] and Griebel and Schweitzer [27] aiming to reduce the linear dependence problem between enriched shape functions constructed through hat-functions in the Particle-Partition of Unity Method. Besides these, with the same objective Babuška et al. [28] employed flat-top PoU to study GFEM superconvergence points.

Zhang et al. [17] propose the following relations to construct a regularized k-degree flat-top PoU in the one-dimensional finite element $e_j := [x_j, x_{j+1}]$,

$$\varphi_1^{e_j}(x) = \begin{cases} 1 & \text{for } x \in [x_j, x_j + \sigma h] \\ \left(1 - \left(\dfrac{x - x_j - \sigma h}{(1 - 2\sigma)h}\right)^k\right)^k & \text{for } x \in [x_j + \sigma h, x_j + (1 - \sigma)h] \\ 0 & \text{for } x \in [x_j + (1 - \sigma)h, x_{j+1}] \end{cases}$$

$$\varphi_2^{e_j}(x) = \begin{cases} 1 & \text{for } x \in [x_j, x_j + \sigma h] \\ 1 - \left(1 - \left(\dfrac{x - x_j - \sigma h}{(1 - 2\sigma)h}\right)^k\right)^k & \text{for } x \in [x_j + \sigma h, x_j + (1 - \sigma)h] \\ 0 & \text{for } x \in [x_j + (1 - \sigma)h, x_{j+1}] \end{cases}$$

(16)

where, $\varphi_1^{e_j}$ and $\varphi_2^{e_j}$ are associated with the left and right nodes, respectively, of the element e_j. The σ parameter defining the flat region size is contained in the range $0 \leq \sigma < 0.5$ and the parameter $k \in \mathbb{N}^*$ controls the smoothness of the curve that connects the flat regions. Zhang et al. [17] also perform numerical analysis on one-dimensional problems and prove that flat-top PoU guarantees stability due to good matrix conditioning.

Sato [18] and Sato et al. [19] through tensorial product of the 1-D relations extend the flat-top PoU formulation to quadrilateral finite elements, and present results that indicate its effectiveness for well controlling matrix conditioning. The Figure 1 illustrates the flat-top PoU defined for quadrilateral finite elements presented by Sato [18] and Sato et al. [19].

Figure 1. Two-dimensional flat-top PoU representation in quadrilateral finite elements, for $\sigma = 0.25$, $k = 1$ and $h = 2$.
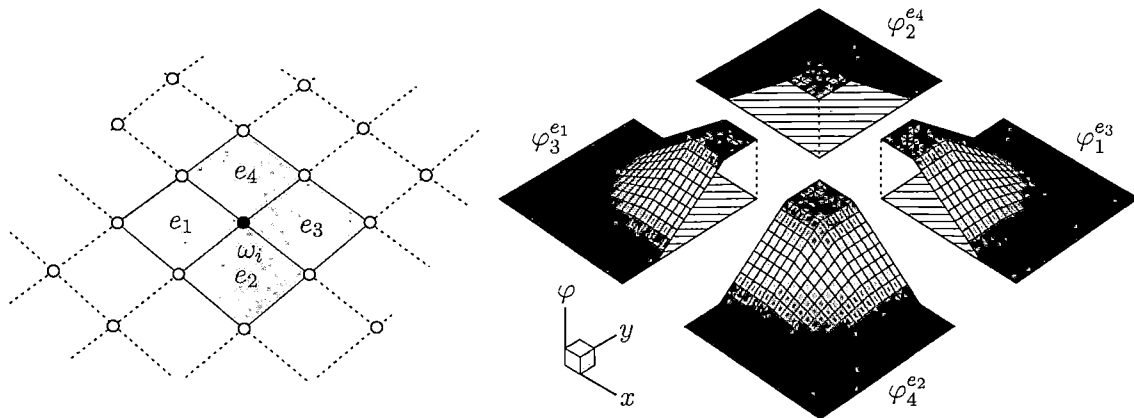
However, Ramos [21] demonstrates that the use of flat-top PoU, despite generating an almost orthogonal enrichment space in relation to the FEM approximation space, demands a complex integration procedure and higher computational cost. Moreover, aiming to provide higher order of continuity, considering the one-dimensional master finite element $\hat{e} := [-1, 1]$, the following PoU is proposed:

$$\varphi_1(\xi) = \cos^2\left(\frac{(1+\xi)\pi}{4}\right), \quad \varphi_2(\xi) = \sin^2\left(\frac{(1+\xi)\pi}{4}\right), \tag{17}$$

where, $\xi \in [-1, 1]$ and φ_1, φ_2 refer to the left and right nodes of the master finite element, respectively. The functions presented in Equation (17) are PoU, once for $\varphi_1(\xi) + \varphi_2(\xi) = 1$.

The trigonometric PoU described in Equation (17) can be understood as a regularization of the flat-top PoU of Equation (16) when $\sigma \to 0$ and keeping its derivative null at the *patch* boundaries. It is emphasized that both trigonometric and flat-top PoU respect this property.

The extension of trigonometric PoU to quadrilateral domain finite element $[-1, 1] \times [-1, 1]$ (see Figure 2) follows from the tensorial product $\varphi_i(\xi) \times \varphi_j(\eta)$,

$$\varphi_1(\xi, \eta) = \cos^2\left(\frac{(1+\xi)\pi}{4}\right) \cos^2\left(\frac{(1+\eta)\pi}{4}\right),$$

$$\varphi_2(\xi, \eta) = \sin^2\left(\frac{(1+\xi)\pi}{4}\right) \cos^2\left(\frac{(1+\eta)\pi}{4}\right),$$

$$\varphi_3(\xi, \eta) = \sin^2\left(\frac{(1+\xi)\pi}{4}\right) \sin^2\left(\frac{(1+\eta)\pi}{4}\right), \tag{18}$$

$$\varphi_4(\xi, \eta) = \cos^2\left(\frac{(1+\xi)\pi}{4}\right) \sin^2\left(\frac{(1+\xi)\pi}{4}\right).$$

Figure 2. Trigonometric PoU representation for quadrilateral finite element.
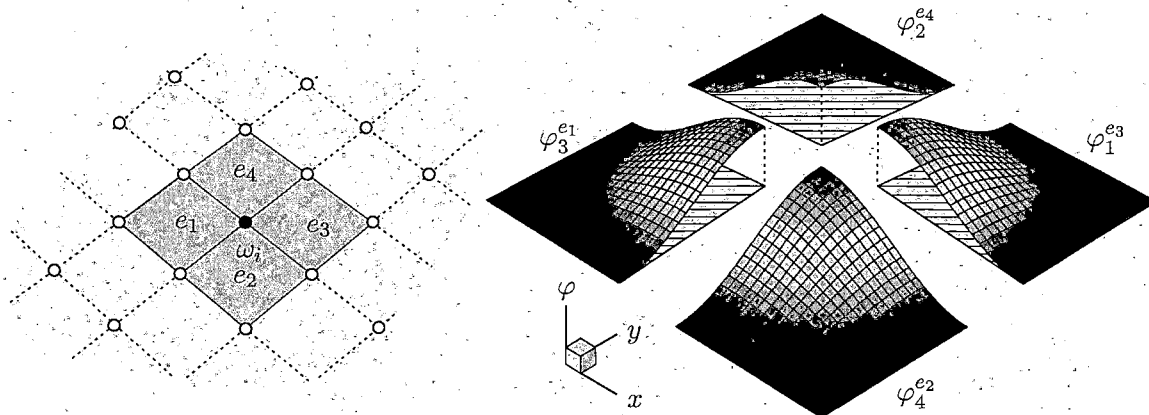

4 Numerical examples and discussion

Let be considered a cracked $\bar{\Omega} = [-a, a]^2$ two dimensional domain with unit thickness and dimension $a = 0.5$. The crack tip $\Gamma_C = \{x : -0,5 \le x \le 0,0, \ y = 0,0\}$ is located at the point $C = (0, 0)$ (see Figure 3). A state of plane strain is considered, as well an elastic linear behavior material with longitudinal modulus of elasticity $E = 1,0$ and Poisson's ratio $\nu = 0.3$.

The loading refers to the first term of asymptotic expansion which represents Mode I of the exact solution of the crack problem in infinite domain, for more details check Szabó and Babuška [29]. It is also

noted that the loading is self-balancing, and its choice of loading allows the representation of the exact solution of the problem. Pointwise restrictions were imposed to eliminate rigid body displacements.

Figure 3. Panel representation with edge crack.
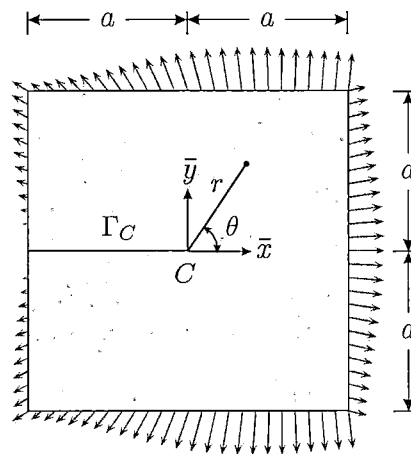
To represent the displacement discontinuity across the crack line, two strategies were employed. Firstly double nodes were used. Therefore the meshes are such that the element borders match the crack line. Secondly, the Heaviside function was adopted to account for the crack opening. In this case the mesh is such that the crack line crosses the elements.

In the discretization six uniform quadrilateral finite element meshes are considered. The geometry of finite element meshes depends on the strategy used to describe the displacement discontinuity present in Γ_C. Thus, in the first group of numerical experiments double knot strategy is employed and singular enrichment is adopted to account for displacement discontinuity. The elements have dimension $h = a/2^i$, $i = 1, 2, \ldots, 6$, leading to mesh grid with $2^{(i+1)} \times 2^{(i+1)}$ cells. In the second group of experiments, which combine the Heaviside function and singular functions to represent the displacement discontinuity, the elements have a dimension $h = 1/\left(2^{(i+1)} + 1\right)$, $j = 1, 2, \ldots, 6$, generating mesh grid of $\left(2^{(i+1)} + 1\right) \times \left(2^{(i+1)} + 1\right)$ cells. For convenience, the first group of meshes will be referred to as *even* and the second as *odd*. As an example, in Figure 4 illustrates the geometry of the quadrilateral finite element mesh of dimension $h = 1/8$ and $h = 1/9$.

Figure 4. Finite element discretization of dimension $h = 1/8$ and $h = 1/9$, respectively . (a) *Even* mesh. (b) *Odd* mesh.

(a)   (b)
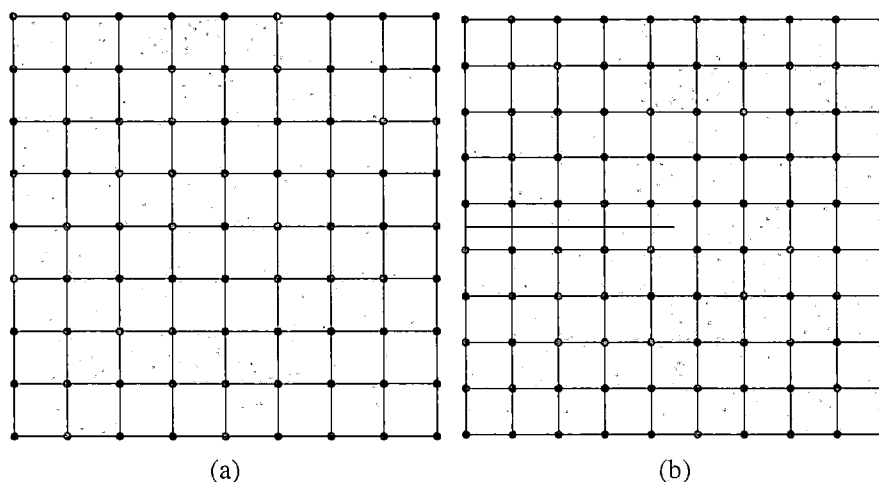
It is also emphasized that the evaluated problems have analytical solution for the displacements (u) and for tensions (σ), Therefore, the approximate solution convergence assessment is based on the measurement of the relative error in the energy norm ϵ^h, being described as

$$\epsilon^h = \frac{\|e^h\|_\Omega}{\|u\|_\Omega} = \frac{\|u - u^h\|_\Omega}{\|u\|_\Omega} = \frac{\sqrt{\int_\Omega (\sigma - \sigma^h)^T \mathfrak{C}^{-1}(\sigma - \sigma^h)d\Omega}}{\sqrt{\int_\Omega \sigma^T \mathfrak{C}^{-1}\sigma d\Omega}}, \tag{19}$$

where, Ω refers to the problem domain, u^h and σ^h are, respectively, the approximate solution obtained for displacements and stresses, $\|u\|_\Omega$ is the displacement measure in energy norm, and $\|e^h\|_\Omega$ indicates the error measure in energy norm.

As already mentioned, the system of equations of GFEM, and its other versions, can be linearly dependent. Thus, to find a solution in the analyzes described throughout this chapter in situations where the stiffness matrix presented a bad condition, the matrix preconditioner proposed by Strouboulis et al. [30]. This strategy consists of applying a small perturbation to the scaled stiffness matrix and iteratively correcting the approximate solution obtained from the succesive system of equations.

It is also noteworthy that in the numerical simulations using the flat-top PoU defined by Sato [18] and Sato et al. [19], the value 0.1 for the parameter σ was adopted, as recommended by those authors.

4.1 Enrichment strategy I

In order to obtain an optimal convergence rate for the cracked domain problem, that is, $\mathcal{O}(h)$, In this section we evaluate the solutions provided by the GFEM versions when only singular enrichment functions aiming to represent the exact solution near the crack tip. So, be Γ_C a crack with the tip located at C, Oden and Duarte [23] and Duarte et al. [31] suggest the use of such a set of functions as enrichment for the displacement field capable of representing the singular behavior of the stresses near the C. Such functions are defined as,

$$L^{S,\bar{x}} = \left\{ \sqrt{r}\left[\left(\kappa - \frac{1}{2}\right)\cos\frac{\theta}{2} - \frac{1}{2}\cos\frac{3\theta}{2}\right], \sqrt{r}\left[\left(\kappa + \frac{1}{2}\right)\sin\frac{\theta}{2} - \frac{1}{2}\sin\frac{3\theta}{2}\right] \right\}$$
$$L^{S,\bar{y}} = \left\{ \sqrt{r}\left[\left(\kappa + \frac{3}{2}\right)\sin\frac{\theta}{2} + \frac{1}{2}\sin\frac{3\theta}{2}\right], \sqrt{r}\left[\left(\kappa - \frac{3}{2}\right)\cos\frac{\theta}{2} + \frac{1}{2}\cos\frac{3\theta}{2}\right] \right\} \tag{20}$$

where, (r, θ) is the polar coordinate system defined according to local cartesian coordinates $(\bar{x}, \bar{y})$ located at the crack tip Γ_C (see Figure 3), $\kappa = (3 - 4\nu)$ (for a state of Plane Strain) and ν is the Poisson's ratio. Still from Equation (20), $L^{S,\bar{x}}$ and $L^{S,\bar{y}}$ are used to enrich the approximation according to local directions $\bar{x}$ and $\bar{y}$, respectively. In short, the singular enrichment vector is defined by:

$$L^S = \begin{cases} L^{S,\bar{x}} \text{ in direction } \bar{x}, \\ L^{S,\bar{y}} \text{ in direction } \bar{y}. \end{cases} \tag{21}$$

Thus, the enrichment vector L^S is used, described in Equation (21), locally in the vicinity of the crack tip. The enrichment zone is limited by a circular region $B(C, R)$, where C is the position of the crack tip and the radius $R = 0,25$ is constant and independent of h (see Figure 5). The set with the indexes of the nodes enriched by the vector L_i^S is then defined as follows,

$$I_h^S = \{i \in I_h : x_i \in B(C, R)\}. \tag{22}$$

where $x = (x, y)$. This enrichment strategy, known as *geometric enrichment* is used, for example, in Fries and Belytschko [4], Gupta et al. [13] and Gupta et al. [14]. In fact, Gupta et al. [13] and Gupta et al. [14] demonstrate that, for GFEM, this strategy provides optimal convergence rates, however the stiffness matrix condition number still presents increasing rate of $\mathcal{O}(h^{-4})$.

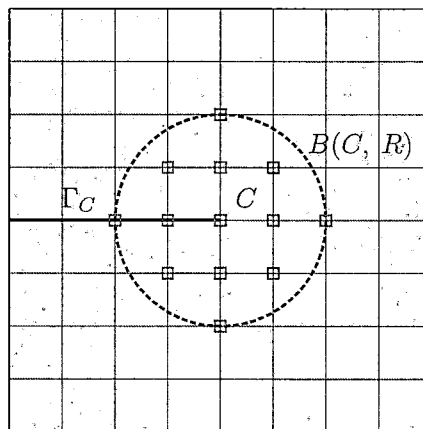Figure 5. Scheme of the enrichment zone. "□" represents nodes enriched by the set of singular functions.

Figure 6 shows that the GFEM presents optimal convergence rate $\mathcal{O}(h)$ while SGFEM, SGFEM^{FT} and SGFEM^{TRIG} reveals convergence rates remaining around $\mathcal{O}(\sqrt{h})$. On the other hand, it is observed that the condition number of GFEM grows with order of $\mathcal{O}(h^{-4})$ whereas for the other versions the results indicate increasing rate order of $\mathcal{O}(h^{-2})$. In fact, *Classical* SGFEM does not provide optimal convergence rate if the same enrichments adopted in GFEM are used. According to Ndeffo et al. [32] and Sanchez-Rivadeneira and Duarte [33], this is because the approximation spaces of GFEM and SGFEM are different, even when adopting both enrichments. Moreover, although SGFEM presents optimal convergence order in the experiment performed, Zhang et al. [15] demonstrates mathematically that this condition cannot be guaranteed in any situation. Still according to these authors, the use of L^S on nodes belonging to I_h^S is sufficient to approximate the singular behavior of the solution, however, it is not efficient to approximate displacement discontinuity in Γ_C.

Figure 6. Enrichment with L^S. (a) Relative error in energy norm. (b) Scaled condition number.

(a)   (b)
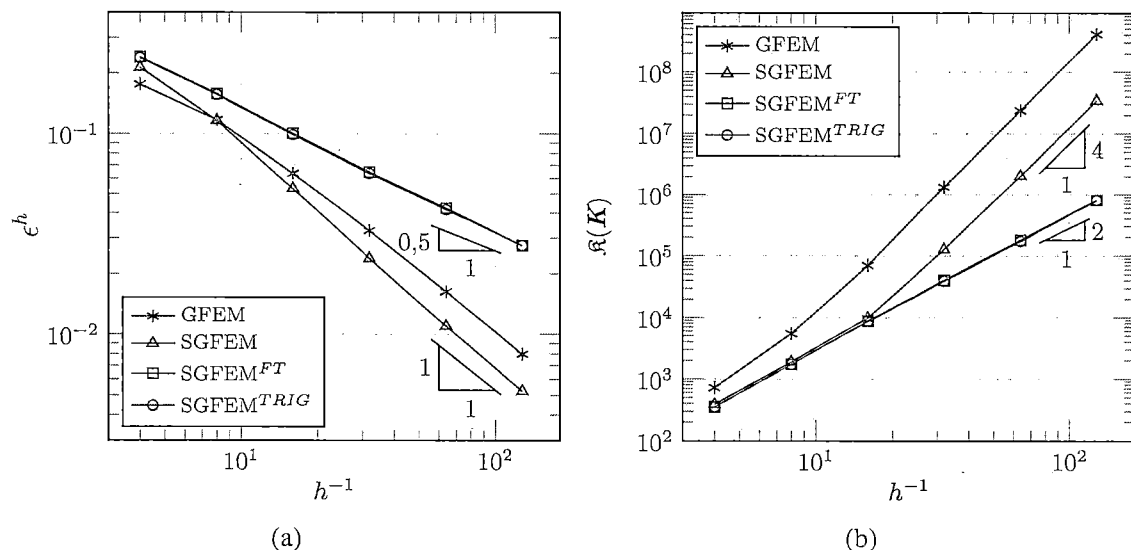
In order to obtain optimal convergence order, additional enrichments were employed in the SGFEM, SGFEM^{FT} and SGFEM^{TRIG}. So, be

$$I_h^{\Gamma_C} = \{i \in I_h : x_i \in e_s \text{ and } e_s \cap \Gamma_C \neq \varnothing\}, \tag{23}$$

the set with the node indexes of the elements e_s intercepted by the crack Γ_C. The strategy used is to add the following terms to the approximation space of such versions of SGFEM,

$$L_i^{SL} = \left\{ L^S \left(\frac{x - x_i}{h} \right), L^S \left(\frac{y - y_i}{h} \right) \right\}, \tag{24}$$

where $i \in I_h^S \cap I_h^{\Gamma_C}$ (see Figure 7). This set of functions will be referred to throughout the paper by function *Singular Linear*. In fact, Sanchez-Rivadeneira and Duarte [33] demonstrate that the use of this set of functions retrieves the optimal convergence rate of the SGFEM cracked domain problem in triangular finite element discretization, however, demonstrate that this strategy can generate dependences between L^S and L^{SL}. In fact, the conditioning problem indicated by these authors was observed after direct application of L^{SL}, as depicted in Figure 8. It can be observed that the use of these additional enrichments provided an optimal convergence order $\mathcal{O}(h)$ in all versions of SGFEM, however, led to loss of stability in relation to matrix conditioning. In particular, it is noted that such strategy generated a growth rate of the scaled condition number of the order of $\mathcal{O}(h^{-8})$, that is, much higher than that obtained even in the GFEM, which is of the order of $\mathcal{O}(h^{-4})$.

Figure 7. Scheme of enrichment zones for SGFEM and other versions. "□" represents the nodes belonging to J_h^1 and "●" the enriched nodes belonging to J_h^2.
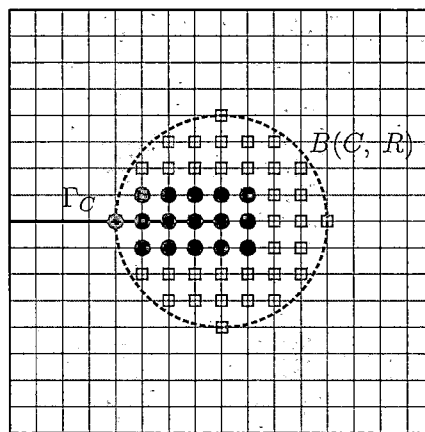
Through the Figure 6b it is noticed that the modification imposed in *Classical* SGFEM did not guarantee stability of the stiffness matrix conditioning and, once adding L^{SL} there is a worsening of this scenario. Thus, in search of a strategy that avoids the presence of linear dependencies between the enrichment functions themselves, a new modification on the space of the SGFEM^{FT} and SGFEM^{TRIG} is hereby proposed. Essentially, a mixed use of the flat-top or trigonometric PoU will be explored. So, be

$$J_h^1 = I_h^S \setminus I_h^{\Gamma_C} \text{ e } J_h^2 = I_h^S \cap I_h^{\Gamma_C}, \tag{25}$$

the SGFEM$_{MD}^{FT}$ and SGFEM$_{MD}^{TRIG}$ approach spaces are defined as,

$$\mathcal{S} = \sum_{i \in I_h} \varphi_i b_0^{[i]} + \sum_{i \in J_h^1} \varphi_i \left(L_i^{\mathcal{S}} - \mathcal{I}_{\omega_i}(L_i^{\mathcal{S}}) \right) b_i^{\mathcal{S}} + \sum_{i \in J_h^2} \varphi_i^* \left(L_i^{\mathcal{S}} - \mathcal{I}_{\omega_i}(L_i^{\mathcal{S}}) \right) b_i^* +$$
$$\sum_{i \in J_h^2} \varphi_i \left(L_i^{\mathcal{SL}} - \mathcal{I}_{\omega_i}(L_i^{\mathcal{SL}}) \right) b_i^{\mathcal{SL}} \tag{26}$$

where φ_i^* represents, depending on the methodology employed, the flat-top or trigonometric PoU and b_i^* are the degrees of freedom related to this PoU. $b_i^{\mathcal{S}}$ and $b_i^{\mathcal{SL}}$ refer to the degrees of freedom linked to singular enrichment and *Singular Linear*, respectively.

Briefly, the idea is to apply the flat-top and trigonometric PoU on $L^{\mathcal{S}}$ only in J_h^2, that is, in the region where the linear parcels of the singular functions are added (see Figure 7).

Therefore, the results illustrated in Figure 8 demonstrate that both the SGFEM_{MD}^{FT} and $\mathrm{SGFEM}_{MD}^{TRIG}$ preserve the optimal convergence order $\mathcal{O}(h)$ and, on top of this, provide a scaled condition number of the order $\mathcal{O}(h^{-2})$, that is, the same order as that obtained from the FEM. Regarding the measurement of the relative error in energy norm, it is observed that the versions of SGFEM^{FT} and SGFEM^{TRIG} present very close results to SGFEM.

Figure 8. Enrichment with $L^{\mathcal{S}}$ and $L^{\mathcal{SL}}$. (a) Relative error in energy norm. (b) Scaled condition number.

(a)   (b)
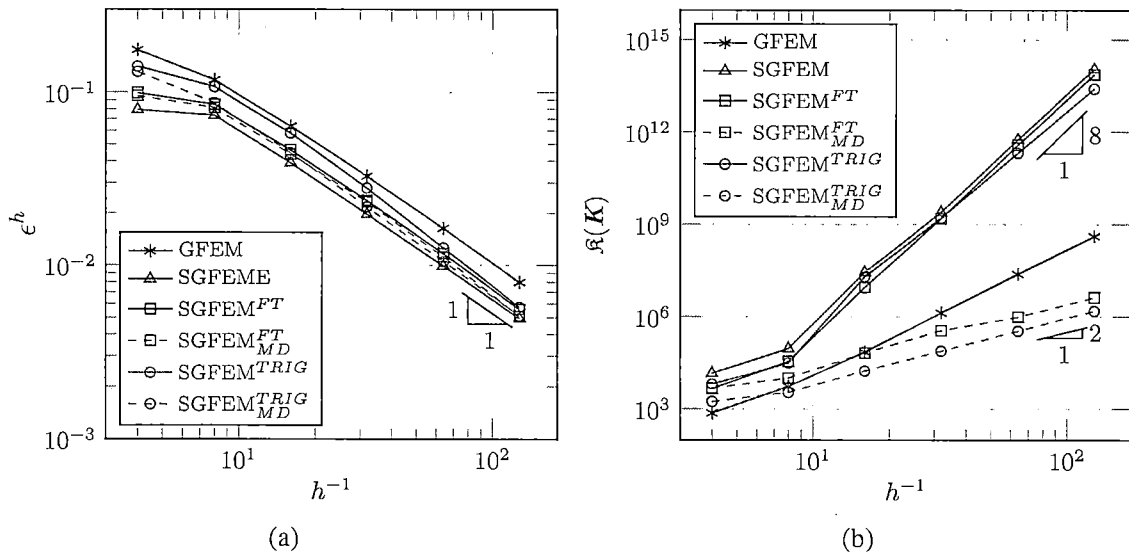
4.2 Enrichment strategy II

This section is to present the behavior of GFEM versions when representing strong discontinuities crossing finite elements. Thus, the Heaviside function is used, which is commonly represented in the literature as follows:

$$\mathcal{H}(x, y) = \begin{cases} 1, & Z(x, y) \geq 0 \\ -1, & Z(x, y) < 0, \end{cases} \tag{27}$$

where $Z(x, y) = 0$ is verified by the crack line. It is mainly intended to evaluate the aspects related to robustness in the considered simulations.

CILAMCE 2019

Proceedings of the XL Ibero-Latin-American Congress on Computational Methods in Engineering, ABMEC.
Natal/RN, Brazil, November 11-14, 2019

Remark 1. According to Babuška et al. [34], the version of GFEM that meets the following properties will be denoted *Robust* SGFEM.
  1. Optimal order of convergence;
  2. Conditioning of stiffness matrix close to that of FEM;
  3. Robutness of the stiffness matrix conditioning in relation to the relative position of the crack to the mesh.

Zhang et al. [15] were the first to point out that the satisfaction of conditions 1 and 2 does not imply the satisfaction of condition 3. In addition, they demonstrate that the modification imposed on the GFEM, defined using Equations (10)–(12), does not generate a *Robust* SGFEM.

Again, we use the vectors of enrichment functions L_i^S, $i \in J_h^1$, and *Singular Linear* L_i^{SL}, $i \in J_h^2$. However, the Heaviside function is added on nodes belonging to J_h^3, where $J_h^3 = I_h^{\Gamma_C} \setminus I_h^S$. Nevertheless, as shown in Gupta et al. [13] and Gupta et al. [14], the modification of the Heaviside function according to the suggestion given by Babuška and Banerjee [1, 2] provides $\mathcal{O}(\sqrt{h})$ convergence rates, so not optimal ($\mathcal{O}(h)$). To restore the convergence rate, Gupta et al. [13] suggest using the function set called *Heaviside Linear*, defined as:

$$L^{\mathcal{HL}}(x,\ y) = \left\{ \mathcal{H}(x,\ y)\frac{(x - x_i)}{h_i},\ \mathcal{H}(x,\ y)\frac{(y - y_i)}{h_i} \right\}. \tag{28}$$

therefore, these parcels were also added to the enrichment in J_h^3 to GFEM, SGFEM^{FT} and SGFEM^{TRIG}. Regarding the enrichment zones, it is observed that $J_h^1 \cap J_h^3 = \varnothing$, i.e., the nodes belonging $B(C,\ R)$ are not enriched by the heaviside function and its linear parcels. The definition of these enrichment zones is in agreement with several works presented in the literature, such as Gupta et al. [13], Gupta et al. [14] and Zhang et al. [15]. For more details, the Figure 9 illustrates the scheme of enrichment regions.

Figure 9. Scheme of enrichment zones for SGFEM, SGFEM^{FT} and SGFEM^{TRIG}. "□" represents the nodes belonging to J_h^1, "•" represents the nodes belonging to J_h^2 and "×" represents the nodes belonging to J_h^3.
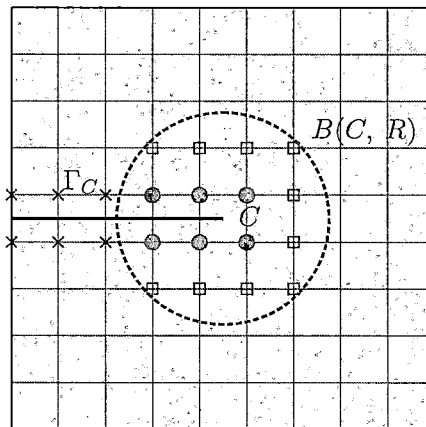

In subsection 4.1 the issue of linear dependence between L^S and L^{SL} in SGFEM was discussed. Therefore, in order to avoid ill conditioning, the analyzes described below the approximation spaces defined in Equation (26) were expanded by including the Heaviside function and its linear parcels. In addition, it is emphasized that the space of the GFEM enrichment functions is defined by the use of L_i^S, $i \in J_h^1$, and the Heaviside function on nodes belonging to J_h^3.

The results obtained are depicted in the Figure 10 and it is observed that all versions of GFEM presented optimal order of convergence, i.e, $\mathcal{O}(h)$. On the other hand, for GFEM and SGFEM, from mesh refinement $h = 1/9$ on, the scaled condition number strats growing by approximately $\mathcal{O}(h^{-4})$. Meanwhile, the conditioning of the stiffness matrix attached to the SGFEM^{FT} and SGFEM^{TRIG} has stable

behavior of $\mathcal{O}(h^{-2})$ throughout the analysis. It is also noted that the SGFEM^{TRIG} presented results closer to those obtained in SGFEM, thus evidencing a better accuracy in relation to SGFEM^{FT}. These results demonstrate that, for the analysis performed, SGFEM^{FT} and SGFEM^{TRIG} can be considered a *Robust* SGFEM as they meet all the conditions described in Remark 1.

Figure 10. Enrichment with $\mathcal{H}$, $L^{\mathcal{HL}}$, L^S e L^{SL}. (a) Relative error in energy norm. (b) Scaled condition number.

(a)   (b)
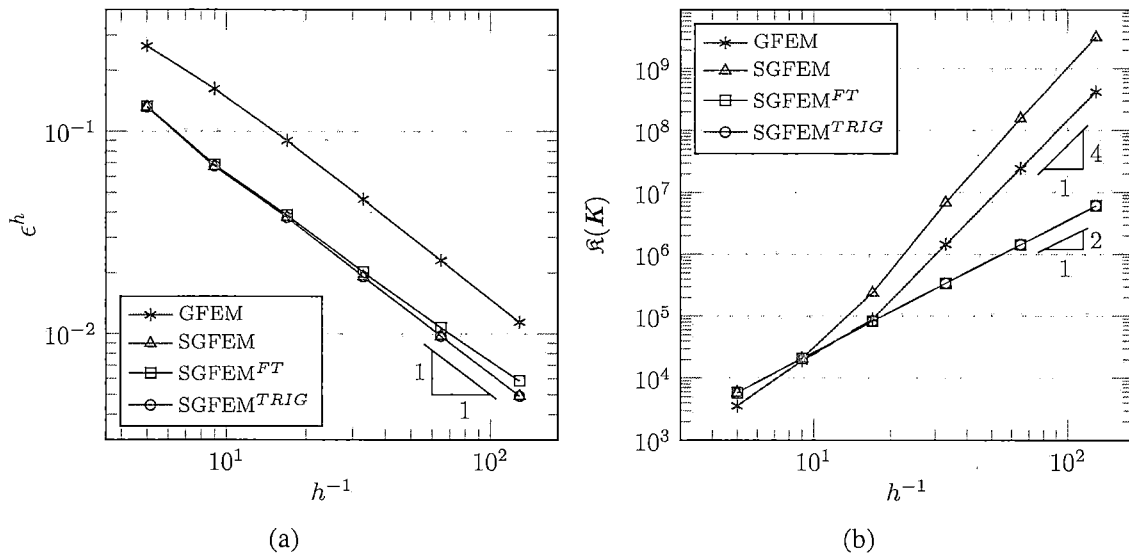
5   Conclusion

In this work, new versions of GFEM have been numerically tested by combining singular enrichment functions and purely discontinuous functions. In particular, the main line of investigation was to evaluate the effect of the modifications employed on *Classical* SGFEM with respect to the matrix conditioning and the order of convergence of the relative error in energy norm. The main contributions are summarized below.

Based on the results presented, it can be seen that in fact the use of flat-top PoU in the space of approximation of enrichment functions provided, in most of the evaluated experiments, the control of matrix conditioning. Similarly, it was observed that trigonometric PoU also played an important role in controlling the scaled condition number of the stiffness matrix. In particular, it is clear that, at this point, the results obtained using this PoU were in good accordance with those presented by the SGFEM^{FT}. This information demonstrates that trigonometric PoU provides good matrix conditioning, in addition requiring a lower computational cost when compared to flat-top PoU.

Regarding the order of convergence of the error, compared to SGFEM the measurement of the relative error in energy norm obtained in the SGFEM^{FT} and SGFEM^{TRIG} is higher, as expected. However, the convergence rate for both methods is of the same order as that obtained in SGFEM.

In addition, the selection strategy presented, in which one chooses which enrichment to combine to each PoUs, has proved to be an efficient alternative for maintaining of the scaled condition number of the order of $\mathcal{O}(h^{-2})$, that is, the same obtained for the FEM. Moreover, as observed, the use of this technique guaranteed robustness in relation to the relative position of the crack to the mesh in the horizontal crack fracture domain problem.

Finally, it can be concluded that the use of different PoUs in the GFEM enrichment space is really an effective alternative to keep under control the stiffness matrix conditioning. The results indicate the possibility of further improvement of this technique to enable more accurate solutions.

Acknowledgements

References

[1] Babuška, I. & Banerjee, U., 2011. Stable generalized finite element method (SGFEM). *Technical Report*.

[2] Babuška, I. & Banerjee, U., 2012. Stable generalized finite element method (SGFEM). *Computer Methods in Applied Mechanics and Engineering*, vol. 201, pp. 91–111.

[3] Béchet, E., Minnebol, H., Moës, N., & Burgardt, B., 2005. Improved implementation and robustness study of the X-FEM for stress analysis around cracks. *International Journal for Numerical Methods in Engineering*, vol. 64, n. 8, pp. 1033–105.

[4] Fries, T. & Belytschko, T., 2010. The extended/generalized finite element method: An overview of the method and its applications. *International Journal for Numerical Methods in Engineering*, vol. 84, n. 3, pp. 253–304.

[5] Laborde, P., Pommier, J., Renard, Y., & SalaÜn, M., 2005. High-order extended finite element method for cracked domains. *International Journal for Numerical Methods in Engineering*, vol. 64, n. 3, pp. 354–381.

[6] Menk, A. & Bordas, S. P. A., 2011. A robust preconditioning technique for the extended finite element method. *International Journal for Numerical Methods in Engineering*, vol. 85, n. 13, pp. 1609–1632.

[7] Chessa, J., Wang, H., & Belytschko, T., 2003. On the construction of blending elements for local partition of unity enriched finite elements. *International Journal for Numerical Methods in Engineering*, vol. 57, n. 7, pp. 1015–1038.

[8] Fries, T., 2008. A corrected XFEM approximation without problems in blending elements. *International Journal for Numerical Methods in Engineering*, vol. 75, n. 5, pp. 503–532.

[9] Gracie, R., Wang, H., & Belytschko, T., 2008. Blending in the extended finite element method by discontinuous galerkin and assumed strain methods. *International Journal for Numerical Methods in Engineering*, vol. 74, n. 11, pp. 1645–1669.

[10] Tarancón, J. E., Vercher, A., Giner, E., & Fuenmayor, F. J., 2009. Enhanced blending elements for XFEM applied to linear elastic fracture mechanics. *International Journal for Numerical Methods in Engineering*, vol. 77, n. 1, pp. 126–148.

[11] Shibanuma, K. & Utsunomiya, T., 2009. Reformulation of XFEM based on PUFEM for solving problem caused by blending elements. *Finite Elements in Analysis and Design*, vol. 45, n. 11, pp. 806–816.

[12] Aragón, A. M., Duarte, C. A., & Geubelle, P. H., 2010. Generalized finite element enrichment functions for discontinuous gradient fields. *International Journal for Numerical Methods in Engineering*, vol. 82, n. 2, pp. 242–268.

[13] Gupta, V., Duarte, C. A., Babuška, I., & Banerjee, U., 2013. A stable and optimally convergent generalized FEM (SGFEM) for linear elastic fracture mechanics. *Computer Methods in Applied Mechanics and Engineering*, vol. 266, pp. 23–39.

[14] Gupta, V., Duarte, C. A., Babuška, I., & Banerjee, U., 2015. Stable GFEM (SGFEM): Improved conditioning and accuracy of GFEM/XFEM for three-dimensional fracture mechanics. *Computer Methods in Applied Mechanics and Engineering*, vol. 289, pp. 355–386.

[15] Zhang, Q., Babuška, I., & Banerjee, U., 2016. Robustness in Stable Generalized Finite Element Methods (SGFEM) applied to Poisson problems with crack singularities. *Computer Methods in Applied Mechanics and Engineering*, vol. 311, pp. 476–502.

[16] Zhang, Q., Banerjee, U., & Babuška, I., 2019. Strongly Stable Generalized Finite Element Method (SSGFEM) for a non-smooth interface problem. *Computer Methods in Applied Mechanics and Engineering*, vol. 344, pp. 538–568.

[17] Zhang, Q., Banerjee, U., & Babuška, I., 2014. Higher order stable generalized finite element method. *Numerische Mathematik*, vol. 128, n. 1, pp. 1–29.

[18] Sato, F. M., 2017. Numerical experiments with stable versions of the Generalized Finite Element Method. Master's thesis, São Carlos School of Engineering, University of São Paulo, São Carlos.

[19] Sato, F. M., Piedade Neto, D., & Proença, S. P. B., 2018. Numerical experiments with the Generalized Finite Element Method based on a flat-top Partition of Unity. *Latin American Journal of Solids and Structures*, vol. 15.

[20] Ramos, C. S. & Proença, S. P. B., 2018. Sobre o emprego da partição da unidade flat-top no MEFG. In *XIII SIMMEC 2018*, Vitória, BR.

[21] Ramos, C. S., 2019. Flat-top and trigonometric Partitions of Unity in the Generalized Finite Element Method. Master's thesis, São Carlos School of Engineering, University of São Paulo, São Carlos.

[22] Proença, S. P. B., 2010. *Introdução aos Métodos Numéricos*. São Carlos, SP.

[23] Oden, J. T. & Duarte, C. A., 1997. Clouds, cracks and FEM's. *Recent Developments in Computational and Applied Mechanics*, pp. 302–321.

[24] Melenk, J. M., 1995. *On Generalized Finite Element Methods*. Ph.d. thesis, University of Maryland.

[25] Griebel, M. & Schweitzer, M. A., 2002. A particle-partition of unity method - Part II: Efficient cover construction and reliable integration. *SIAM Journal on Scientific Computing*, vol. 23, n. 5, pp. 1655–1682.

[26] Schweitzer, M. A., 2003. *A Parallel Multilevel Partition of Unity Method for Elliptic Partial Differential Equations*. Number 29 in Lecture Notes in Computational Science and Engineering. Springer, Berlin, Heidelberg, 1 edition.

[27] Griebel, M. & Schweitzer, M. A., 2007. A Particle-Partition of Unity Method - Part VI: Adaptivity. In Griebel, M. & Schweitzer, M. A., eds, *Meshfree Methods for Partial Differential Equations III*, number 57 in Lecture Notes in Computational Science and Engineering, pp. 121–147. Springer, Berlin, Heidelberg.

[28] Babuška, I., Banerjee, U., & Osborn, J. E., 2007. Superconvergence in the generalized finite element method. *Numerische Mathematik*, vol. 107, n. 3, pp. 353–395.

[29] Szabó, B. & Babuška, I., 1991. *Finite Element Analysis*. John Wiley and Sons, New York.

[30] Strouboulis, T., Babuška, I., & Copps, K., 2000. The design and analysis of the generalized finite element method. *Computer Methods in Applied Mechanics and Engineering*, vol. 181, n. 1-3, pp. 43–69.

[31] Duarte, C. A., Babuška, I., & Oden, J. T., 2000. Generalized finite element methods for three-dimensional structural mechanics problems. *Computers & Structures*, vol. 77, n. 2, pp. 215–232.

[32] Ndeffo, M., Massin, P., Moës, N., Martin, A., & Gopalakrishnan, S., 2017. On the construction of approximation space to model discontinuities and cracks with linear and quadratic extended finite elements. *Advanced Modeling and Simulation in Engineering Sciences*, vol. 4, n. 1, pp. 6.

[33] Sanchez-Rivadeneira, A. G. & Duarte, C. A., 2019. A stable generalized/extended FEM with discontinuous interpolants for fracture mechanics. *Computer Methods in Applied Mechanics and Engineering*, vol. 345, pp. 876–918.

[34] Babuška, I., Banerjee, U., & Kergrene, K., 2017. Strongly stable generalized finite element method: Application to interface problems. *Computer Methods in Applied Mechanics and Engineering*, vol. 327, pp. 58–92.